Title: Cu and Zr surface sites in photocatalytic activity of TiO_2 nanoparticles: The effect of Zr distribution

Authors: Olena Pliekhova, Oleksii Pliekhov, Mattia Fanetti, Iztok Arcon, Natasa Novak Tusar, Urska Lavrencic Stangar

PII: S0920-5861(18)30819-8
DOI: https://doi.org/10.1016/j.cattod.2019.01.022
Reference: CATTOD 11893

To appear in: *Catalysis Today*

Received date: 23 June 2018
Revised date: 21 December 2018
Accepted date: 7 January 2019

Please cite this article as: Pliekhova O, Pliekhov O, Fanetti M, Arcon I, Tusar NN, Stangar UL, Cu and Zr surface sites in photocatalytic activity of TiO_2 nanoparticles: The effect of Zr distribution, *Catalysis Today* (2019), https://doi.org/10.1016/j.cattod.2019.01.022

Cu and Zr surface sites in photocatalytic activity of TiO_2 nanoparticles: the effect of Zr distribution

Olena Pliekhova[1], *Oleksii Pliekhov*[2], *Mattia Fanetti*[1], *Iztok Arcon*[1,3], *Natasa Novak Tusar*[2,1], *Urska Lavrencic Stangar*[4,1*]

[1]University of Nova Gorica, Vipavska 13, SI-5000 Nova Gorica, Slovenia

[2]National Institute of Chemistry, Hajdrihova 19, SI-1000 Ljubljana, Slovenia

[3]Jozef Stefan Institute, Jamova 39, SI-1000 Ljubljana, Slovenia

[4]University of Ljubljana, Faculty of Chemistry and Chemical Technology, Vecna pot 113, SI-1000 Ljubljana, Slovenia

[*]*Urska.Lavrencic.Stangar@fkkt.uni-lj.si*

Graphical Abstract

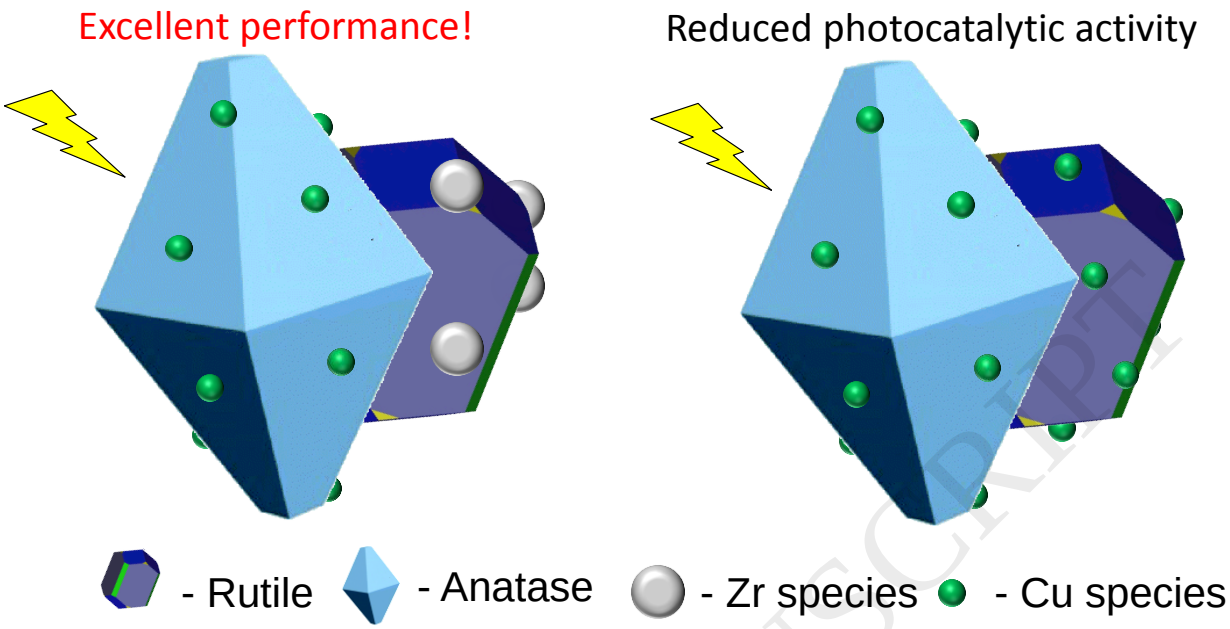

Highlights

- Zirconium loading improves mechanical properties of TiO_2 photocatalytic layers.
- High coper loading is harmful for photocatalytic performance.
- Combined Cu/Zr modification of mixed phase TiO_2 is beneficial for dye degradation.

Abstract

The present work is focused on the role of ZrO_2 modification in the performance of CuO modified TiO_2. Zirconia loading leads to formation of more resistant photocatalytic layers compared to samples modified with only copper containing species. Surface modification of mixed phase TiO_2 with CuO/ZrO_2 improves the degradation of Reactive blue 19 dye under simulated solar irradiation. An in-depth investigation of the catalysts showed that in case of CuO/ZrO_2 modification, the covering of the TiO_2 surface with zirconium containing species prevents morphological and harmful energetic changes induced by copper species formed on the rutile TiO_2 phase at a higher copper loading.

Keywords: titanium dioxide; surface modification; XAS analysis; surface acidity; Hammett indicators.

Introduction

Despite the progress made in the material chemistry of TiO_2 [1,2] there are still obstacles in using solar light for efficient photocatalytic water purification and disinfection processes. The efficient applicability of TiO_2 for environmental purposes, which is restricted by its limited activity under the solar light, is strongly connected to TiO_2 visible light sensitivity. In the context of TiO_2 limiting application under the solar light, Cu^{2+} ions and CuO have attracted much attention as promising surface modifiers [3-7] since they facilitate the visible light absorption.

According to the work of Ire et al. [6], the visible light sensitivity and enhancement of TiO_2 photocatalytic activity by Cu^{2+} modification can be explained by formation of the mid-level Cu3d states. The mid-level states enable the transition of electrons from the valence band of TiO_2 to the empty CuO states (visible light sensitivity) leading to enhanced electron/hole separation [8,9]. However, the benefits of modifying TiO_2 with copper containing species are not obvious. The efficiency of pollutant degradation under visible and UV light depends strongly on the amount of the grafted species [10-13]. For example, the degradation of 2-naphthol and p-cresol by TiO_2 modified with a small amount of CuO increases, however it decreases with higher amount of CuO loaded [12].

This issue, concerning the loaded amount of CuO species and photocatalytic activity was thoroughly discussed by Jin et al. [12]. The effect that CuO modification has on the energy levels (valence band (VB) and conduction band (CB)) of rutile (110) and anatase (001) TiO_2

surfaces was shown by density functional theory and spectroscopic experiments [12]. The energy of the VB maximum of photocatalyst is important because it determines the ability of the photo generated holes to oxidise organic pollutants [14]. The VB energy increase is leading to formation of holes with weakened oxidative power and as a consequence to lower photocatalytic activity. It was shown that the surface modification of rutile (110) and anatase (001) by the CuO nanoclusters can cause a significant change in the TiO_2 energy bands [12]. It was clear that the change at the VB strongly depends on CuO loading, expressed by means of the elementary $(CuO)_n$ species in the surface supercell utilized for modelling, with n = 1, 2, 4 [12]. The study concluded that at low and high CuO loading two different mechanisms of organic pollutant degradation are possible. The major effect of the CuO modification at low copper loading (n = 1) is the excitation of the electrons from the TiO_2 VB to the unoccupied Cu3d levels as suggested by Ire et al. [6]. Whereas at higher copper loading (n = 2, 4) the upward shift of the VB edge and the excitation from the surface CuO to the CB of TiO_2 – reverse charge localization – is likely dominant. Moreover, it was hypothesised that the type of TiO_2 crystal phase, on which CuO clusters are formed, plays a role in the activity of CuO modified TiO_2. The upward shift of the VB edge at n = 2, 4 for anatase is not as significant as it is for modified rutile [12], therefore the reverse charge localization mechanism is not obvious in this case and, probably, it is shifted towards higher copper loading. The schematic pattern of the reverse charge localization mechanism is presented in Figure 1.

Coupling of TiO_2 and ZrO_2 is claimed to alter the textural and structural characteristics of TiO_2 such as increasing surface acidity, adsorption ability and the active surface area [15], [16]. Additionally, outstanding mechanical properties are inherent to zirconium oxide, and

improved scratch resistance and durability are observed for deposited layers of ZrO_2 modified TiO_2 [17].

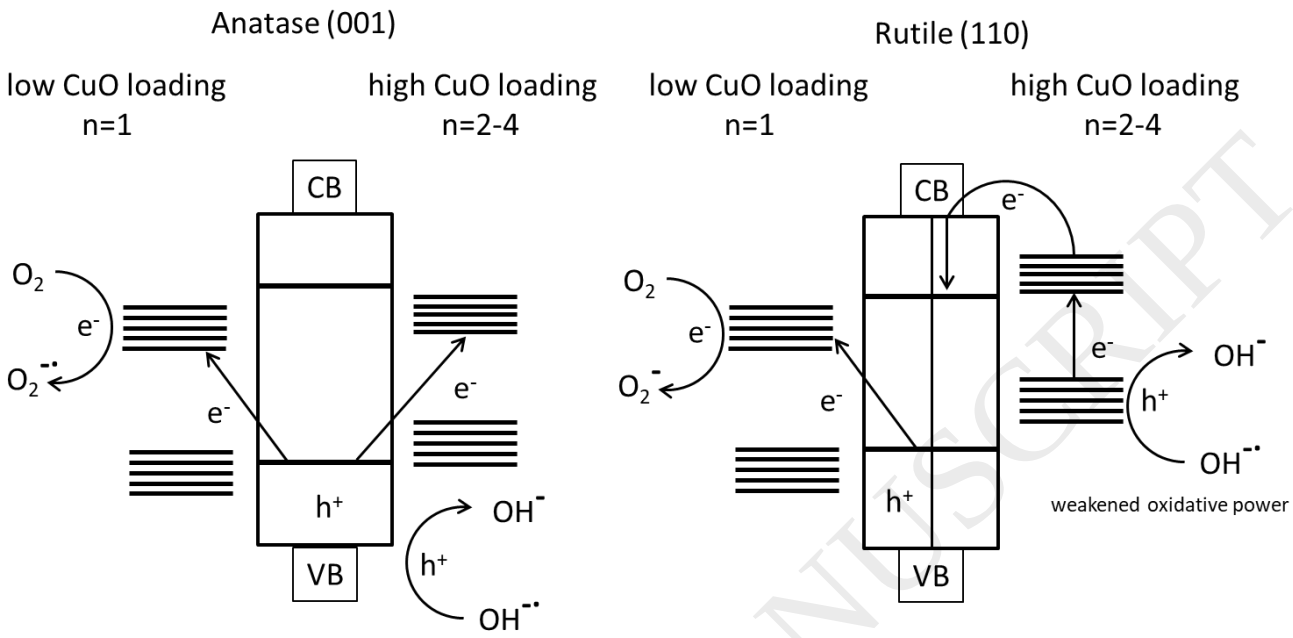

Figure 1. The schematic pattern of the reverse charge localization mechanism on CuO modified rutile TiO_2.

The addition of two different species of metal oxides on the TiO_2 surface opens up new possibilities in the modification of photocatalysts. A synergistic effect is possible if two different transition metal elements are co-loaded to TiO_2 [18]. The positive effects of nickel [19] and silver [20] containing species for copper modified Aeroxide® Degussa P25 titanium dioxide (P25) were observed.

Commercial Aeroxide® Degussa P25 is known as a mixed phase TiO_2 benchmark with high UV-light activity. It contains anatase and rutile phases in a ratio 3:1. It was declared that the synergistic effect between the anatase and rutile is responsible for the high reactivity of P25 [21]. Lately it was shown that rutile is the one which is responsible for the

separating of the electrons from the holes in P25 [22]. Spanos et al. [31] showed that the mixed phase P25 surface consists of rutile and anatase regions with independent acidic behaviour. Using potentiometric titration and a so-called two pK model, it was evident that the surface of rutile is more acidic (pK_1 = 3.9; pK_2 = 6.8) than anatase (pK_1 = 4.6; pK_2 = 8.1) [31]. This gives an opportunity to chemically distinguish between anatase and rutile sites on the surface of P25.

In our previous work [10], we simultaneously used copper and zirconium oxide species as surface modifiers of P25. The results showed positive effect of ZrO_2 on the photocatalytic activity of CuO modified TiO_2 with higher loading of copper containing species. However, the mechanism of this effect stayed unclear.

Herein, we performed the testing of P25 titania with simultaneous copper oxide and zirconium oxide surface modification against the widely used C.I. Reactive blue 19 (RB 19) dye. Dependence of the photocatalytic activity on the zirconium containing species in the CuO modified P25 was observed and a possible mechanism responsible for this effect is discussed.

Materials and methods

Preparation of photocatalysts

Surface modified photocatalysts were prepared by modifying P25 (Aeroxide® Degussa). Organic metal precursors (MP) were used for surface modification. Deionized water prepared with a NANOpure system (Barnstead) was used throughout.

Organic MP were used in combination of sol-gel and impregnation methods. Absolute ethanol (C_2H_5OH), 96% (Sigma-Aldrich), acetylacetone ($C_5H_8O_2$), 99% (Merck), copper(ll) acetyl-acetonate ($C_{10}H_{14}CuO_4$), 99% (Merck), zirconium(lV) butoxide ($Zr(OC_4H_9)_4$), 80%

in 1-butanol (Sigma-Aldrich) were used. All the chemicals were mixed together to obtain a titanium dioxide slurry with 0.05; 0.1; 0.5 mol% of copper, 1 mol% of zirconium, and double metal modified samples with 0.05 and 0.1 mol% of copper and 1 mol% of zirconium. Initially, a calculated amount of MP, copper(ll) acetyl-acetonate (0.008 g; 0.016 g; 0.080 g) and zirconium(lV) butoxide (286 µL), were dissolved in 20 mL of absolute ethanol. Acetylacetone (chelating agent) was added gradually in a molar ratio of MP/$C_5H_8O_2$ = 1/3. Ten times the stoichiometric amount of water to MP was added dropwise. Catalysts modified with both copper and zirconium containing species were prepared by simultaneously adding the required amount of both MP. After 1 h of stirring, 5 g of P25 was added and the slurry stirred for a further 1 h. The slurries were then dried at 80 °C, calcined at 500 °C for 2 h and ground in an agate mortar.

In order to keep clarity and to shorten names of the samples in the article body, Cu symbol represents copper oxide clusters and Zr symbol zirconium oxide clusters. The number following Cu or Zr in sample names determines its molar percent with respect to Ti.

Photocatalytic test

The photocatalytic experiment involved degrading RB19 (model pollutant) in water (initial concentration 50 ppm). The suspension consisted of 0.1 g of photocatalyst in 100 mL of RB19 solution. First, the suspension was sonicated in a cold ultrasonic bath for 10 min. In order to achieve adsorption-desorption equilibrium, the suspension was left for 1 h by stirring in the dark. After equilibration, the suspension was irradiated for 50 min in a solar simulator chamber (Suntest XLS+, Atlas) with a Xenon lamp, using a daylight filter. Irradiation intensity was 75.0 mW/cm^2 (300–800 nm) with UVA fraction of 6.1 mW/cm^2 (300–400 nm). This was repeated for each photocatalyst sample.

The concentration of RB19 in the supernatant was determined using a Perkin Elmer UV/Vis spectrophotometer (wavelength = 594 nm). The percent of RB19 bleaching was estimated using the following equation:

$$RB19\ bleaching\ (\%) = [(C_0 - C)/C_0] \times 100 \qquad (1)$$

where C_0 is the concentration of the RB19 solution before irradiation; C is the concentration of RB19 after 50 min of irradiation. The accuracy of the photoactivity measurements was ± 3%.

The amount of total organic carbon (TOC) was determined using a multi N/C 3100 analyser (Analytik Jena) after 3 h of sample irradiation. Each sample, prior to analysis, was centrifuged to separate out the nanoparticles of TiO_2 from the solution. The solution was acidified manually by adding 2-3 drops of 25% H_2SO_4. Sample incineration temperature was 850 °C with 300 s detector integration time.

Characterization of Cu/Zr-TiO_2 catalysts

The crystal structures of the TiO_2 samples were identified by X-ray diffraction (MiniFlexBenchtop 300/600, 150) using Cu Kα irradiation from 10 to 80 ° at a scan rate of 2 °/min. The phase composition analysis was performed by the Rietveld refinement method (High Score Plus software). The crystallite size was determined by the Scherrer formula:

$$t = 0.9\lambda/(\beta \cos \theta) \qquad (2)$$

where t is particle size in nm, λ the wavelength of the X-ray in Å (1.5418 Å), β full width of the diffraction peak on its half maximum (FWHM) in radians and θ is the Bragg angle.

The actual copper loading was determined by complexometric titration with EDTA according to the procedure available in supplementary materials. The actual zirconium loading was determined by energy dispersive X-ray (EDX) standardless analysis routed by means of field emission scanning electron microscope (JSM – 7100f, JEOL)

equipped with an EDX detector (X-Max80, OXFORD). For making measurements the powders were pressed into pellets.

Scanning transmission electron micrographs were acquired on a JEOL JEM 2100 microscope operated at 200 kV. The powders were dispersed in water and a drop of diluted suspension was placed on a carbon-coated grid and evaporated at ambient temperature.

The surface acidity of the catalysts was determined by titration using n-butylamine following the procedure described in [23]. Four Hammett indicators with different pK_a were used: neutral red (pK_a = +6.8), bromothymol blue (pK_a = +6.0), methyl red (pK_a = +4.4), and methyl yellow (pK_a = +3.3). Each photocatalytic powder (0.1 g) was dispersed in 10 mL of benzene to which were added three drops of an indicator/benzene solution. The contents were stirred using a magnetic Teflon coated stirring bar.

The amount of acid on a solid (A) is expressed as the number of mmol of acid sites per unit weight:

$$A = C \cdot V / m \qquad (3)$$

where C is the concentration of n-butylamine (0.01 M), V is the volume of n-butylamine used for titration, m is the mass of photocatalytic powder.

Detailed information about the calculations is available in the supplementary materials.

In order to prepare films, powders were dispersed in a titanium-silicon binder solution according to the procedure described in [24]. After deposition, the fresh layer was dried with a hair dryer and heat-treated at 150 °C for 30 min. The mechanical stability of one month old films was evaluated using the Hardness Pencil test (also named Wolf-Wilborn test) with an ELCOMETER 501.

EXAFS and XANES spectra of Cu and/or Zr modified TiO_2 samples with varied metal concentrations and reference Cu and Zr compounds were measured in either fluorescence or transmission detection mode with the P65 beamline of the PETRA III (DESY) and the XAFS beamline of Elettra synchrotron radiation facilities. Detailed information is available in the supplementary materials.

The analysis of XANES and EXAFS spectra was performed with the Demeter (IFEFFIT) program package [25] in combination with FEFF6 program code [26] for ab initio calculation of the photoelectron scattering paths.

Results and discussion

A characterization of the materials led to the following major visual observations: the powders loaded with copper are different in colour, becoming more green-brownish with an increasing amount of Cu, while the powders with Zr loading retain their whiteness. The changes in the crystalline structure were examined by X-ray diffractometry (XRD). Only peaks characteristic of the anatase and rutile phases from P25 were observed (Fig. SM1, supplementary materials). The absence of XRD reflections of copper oxide and zirconia crystalline phases in the XRD patterns can be attributed to the low amount and fine dispersion of Cu and Zr containing species on the TiO_2 surface. The unit cell parameters and phase content of the photocatalysts are presented in the supplementary materials (Table SM1).

The loading of Cu, as determined by complexometric titration, is in good agreement with the theoretical value (Table SM1). The loading of Zr, as determined from EDX analysis, is constant in all of the samples but is lower than the nominal 1 mol% (see Table SM1 and its footnote).

Considering that the photocatalysts were developed for water purification purpose, immobilization of the active layers is important. The prepared CuO and ZrO_2 modified TiO_2 powders were mixed with a binder sol and immobilized on glass plates. The results of scratch resistance tests of the Zr/Cu modified TiO_2 layers are presented in Fig. 2.

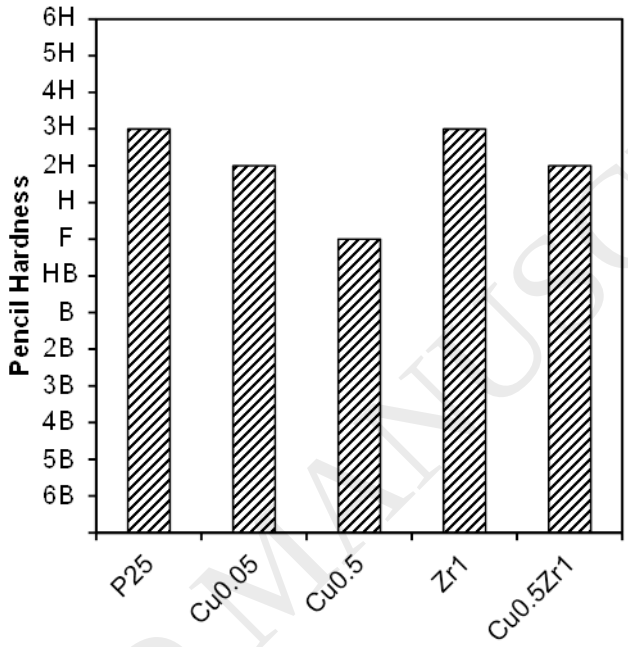

Figure 2. Scratch resistance test of the immobilized layers of the different photocatalysts (6H – the hardest, 6B – the softest pencil).

It is evident, that Cu modification leads to the formation of less resistant coatings. The hardness of the film obtained from the powder with 0.5 mol% of Cu drops by four units compared to a film prepared from unmodified P25. This is a consequence of the agglomeration process observed in the CuO modified samples [10] and resulting porosity of the layers [24]. In contrast, the addition of both ZrO_2 and CuO leads to the formation of more resistant films compared to films containing only Cu species. This means surface modification of copper

modified TiO_2 with zirconium species is beneficial in regards to the mechanical properties of the immobilized layers.

In a previous publication [17], it is stated that an increase in hardness of Zr modified titania films is followed by a decrease in the photocatalytic activity. The degradation of dye under simulated solar light was performed. Figure 3 shows that the highest degree of dye degradation, calculated from the UV-Vis spectroscopy measurements (bleaching, 72%) after 50 min of irradiation and the highest degree of mineralization calculated from the TOC data (83%) after 3 h of irradiation, were recorded for the sample with the lowest (0.05 mol%) copper loading. According to [6], this can be explained by the formation of the mid-level Cu3d states. In this case, upon irradiation an electron is localized at the copper nanocluster and a hole on the TiO_2 surface. The mid-level states enable the transition of electrons from the VB of TiO_2 to the empty CuO states and enhance electron/hole separation [6]. At a higher copper loading a lower level of dye degradation was observed: about 40% of bleaching and 50% of TOC for 0.1 and 0.5 mol% of Cu loading. This result is consistent with the statement about the dependence of photocatalytic activity of Cu modified photocatalysts from the amount of deposited copper oxide [11], [12]. According to [12] the upward band shift causes reverse localization of electrons and holes at higher copper loading, which leads to a weakened oxidation ability of the generated holes.

It is interesting that surface modification with 1 mol% of Zr-only (without copper) does not influence the photocatalytic performance of P25 towards RB19. In fact, in this case about 63% of bleaching and 80% of mineralization is registered, which is within the error range of the result for pristine P25. Our findings do not contradict the findings of

Guerrero-Araque et al. [27] who found that the beneficial defects induced by ZrO_2-TiO_2 heterojunction are not formed at low Zr loading.

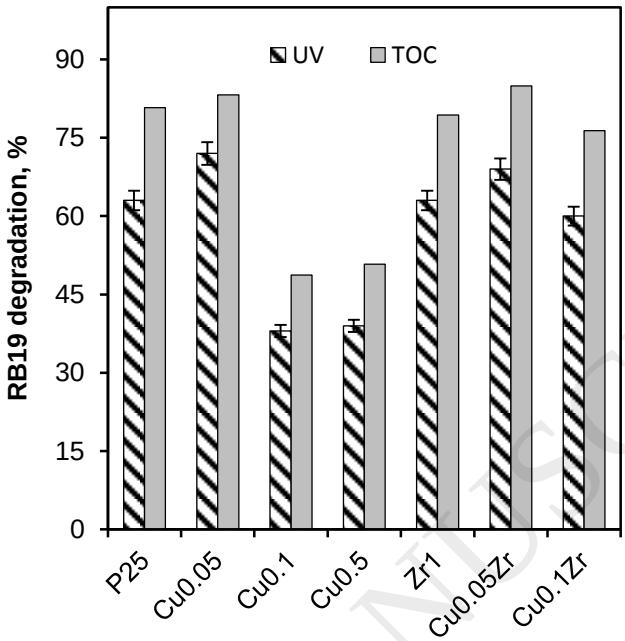

Figure 3. Degradation of RB19 by Cu/Zr modified TiO_2. The UV results correspond to the amount of dye degradation measured by UV-Vis spectroscopy (bleaching) after 50 min of light irradiation; TOC results correspond to the amount of dye mineralization after 3 h of light irradiation.

In the presence of copper, zirconium species play a beneficial role in the efficiency of dye degradation. In the case of low copper loading (0.05 mol%) the influence of Zr on photocatalytic activity is not detected: 69% of bleaching and 85% of TOC decrease for RB19 degradation by Cu/Zr modified sample versus 72% of bleaching and 83% of TOC decrease by a Cu modified sample without added Zr. However, at a higher Cu loading (0.1 mol%), the efficiency of dye degradation of the double metal modified photocatalyst led to 60% bleaching and 76%

reduction in TOC (mineralization) compared to 40% bleaching and 50% reduction in TOC for a copper only modified sample.

To discover the mechanism responsible for this effect a further investigation was performed. It has been pointed out [12] that the chemisorption of copper(II) acetyl-acetonate on the surface of TiO_2 occurs without the elimination of the acetyl-acetonate ligand, which is afterwards eliminated by heating. In this study, the samples were calcined to decompose all of the organic compounds originating from the precursors.

The morphology of the photocatalysts was investigated by electron microscopy. Figure 4 shows a STEM image of a 0.05 mol% Cu modified sample. The presence of bright features of about 1-2 nm size are clearly visible on the surface of TiO_2 nanoparticles. Since in dark-field STEM the intensity in the images increases with the atomic number of the elements, the presence of features brighter than TiO_2 (and not present in the images of unmodified TiO_2) is compatible with the idea of copper-containing nanoclusters. Unfortunately, as a result of limited statistics it was not possible to clearly state the size and/or density increment of the observed CuO features at a higher Cu loading.

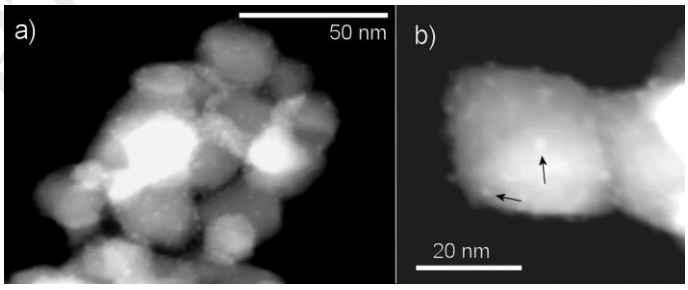

Figure 4. Dark-field scanning transmission electron micrographs of 0.05 mol% Cu modified TiO_2 at different magnifications: a) an agglomeration of nanoparticles; b) CuO nanoclusters on the surface of a TiO_2 nanoparticle identified by arrows.

The large bright features in the centre of the Fig. 4a are not Cu particles, but regions where multiple nanoparticles overlap, which creates a brighter signal. The saturation is due to enhanced contrast, which is necessary to visualize the features in the rest of the picture.

The Cu K-edge XANES analysis was used to determine the Cu valence states in the Cu and Cu/Zr modified P25 photocatalysts. The valence state of the Cu cation is known to directly affect the energy position of the Cu K-edge and pre-edge features ascribed to the (1s-4p) transitions. Changes in the energy of the Cu K-edge and pre-edge features of about 4 eV is observed between Cu(I) and Cu(II) cations [6, 10, 28, 29, 30].

The normalized Cu K-edge XANES spectra of the samples are shown in Fig. SM2 (supplementary materials), together with the XANES spectra of the reference copper compounds with Cu(I) and Cu(II) valence states and a similar Cu coordination. The energy position of the Cu K-edge and pre-edge features in the XANES spectra of the catalyst samples, compared to those in the spectra of the Cu reference compounds, suggest that the oxidation state of copper cations in the samples is Cu(II).

A Cu and Zr K-edge EXAFS analysis is used to determine the average local structure around the Cu and Zr cations in the Cu, Zr and Cu/Zr modified P25 photocatalysts. In Fourier transform EXAFS the magnitude of the Cu (Fig. SM3) and in the Zr K-edge EXAFS spectra of the samples (Fig. 5) the contribution of photoelectron backscattering on the nearest shells of neighbouring atoms around the Cu or Zr atoms are observed as peaks in the R range from 1 to 3.6 Å.

A good agreement is observed between the model (detailed description of the model can be found in supplementary material) and the experimental spectra for all the photocatalysts, using the k range of 2.5 – 11.0 $Å^{-1}$ and in the R range of 1.0 – 3.6 Å for Cu EXAFS spectra (Fig.

SM3), and k and R ranges of 3.0 –13.5 $Å^{-1}$ and 1.0 – 3.7 Å, respectively, for Zr EXAFS spectra (Fig. 5). A list of the best fit parameters is given in the Tables SM2-SM4.

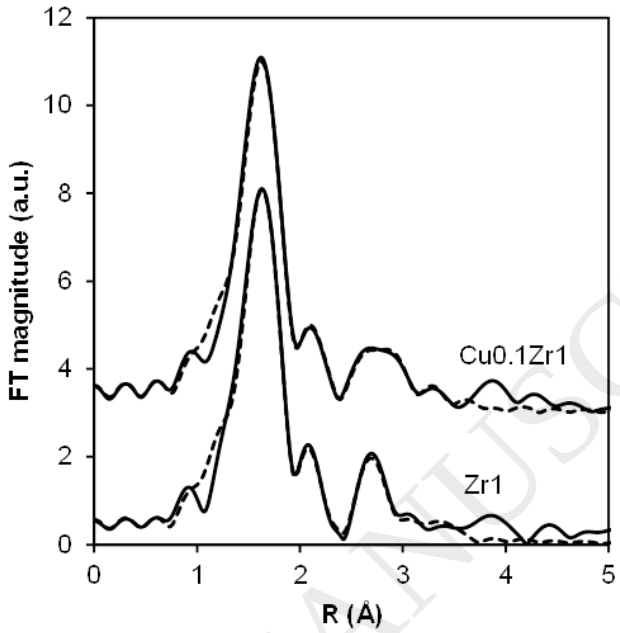

Figure 5. Fourier transform magnitude of k^3-weighted Zr K-edge EXAFS spectra of Zr and Cu/Zr modified P25 photocatalysts, calculated in k and R ranges of 3.0 – 13.5 $Å^{-1}$ and 1.0 – 3.7 Å, respectively. Experiment: solid line; best-fit EXAFS model: dashed line.

Similar average local neighbourhoods of Cu are found in all the photocatalyst samples. The Cu cations are octahedrally coordinated to six oxygen atoms, in a distorted octahedron with four oxygen atoms in the equatorial plane with short Cu-O distances (1.95 –1.98 Å) and two oxygen atoms on axial positions where the Cu-O distances are longer (2.18 –2.28 Å). In the more distant coordination shells, Ti and Cu neighbours are detected, while Zr neighbours are ruled out by the fit. The results show that a portion of Cu cations is bound to the TiO_2 surface

forming Cu-O-Ti connections and a portion of the Cu cations form Cu-O-Cu connections.

The average Cu neighbourhood is mostly independent of Cu loading in Cu or in Cu/Zr modified photocatalysts, except at high Cu loadings (1% and 3%), where the average numbers of Cu and Ti neighbours are found to be slightly lower, compared to those in photocatalysts with lower Cu loadings. The result suggests that CuO nanoparticles are formed on the TiO_2 surface. In the Cu/Zr modified P25 photocatalysts, there are no Cu-O-Zr bonds, which indicates that separate ZrO_2 and CuO species are formed on the TiO_2 surface.

The result is supported also by Zr EXAFS analysis (Table SM5), which shows that the Zr cations in Cu/Zr modified P25 photocatalyst are dispersed on the surface of TiO_2 as ZrO_2 nanoparticles bonded to the TiO_2 surface. Average Zr local neighbourhood in Cu/Zr modified P25 is similar to that found in the Zr only modified P25 photocatalyst. In both cases Zr-O-Zr and Zr-O-Ti bonds are present, but there are no Zr-O-Cu connections.

According to the results obtained from the X-ray absorption spectroscopy and further assessed by STEM-EDX mapping (Fig. 6) it can be summarized that Zr and Cu containing species do not form mixed clusters and are homogeneously distributed on the TiO_2 surface. These results and the assumption that the type of TiO_2 crystal phase, on which CuO clusters are formed, plays a role in the activity of CuO modified TiO_2 [12] led us to the hypothesis about hindering the rutile surface sites by ZrO_2 in the mixed phase TiO_2. Our hypothesis suggests that the hindering of rutile surface sites by ZrO_2 leads to increased photocatalytic activity of the Cu/Zr modified sample compared to the sample with the same amount of Cu loaded, but distributed on both TiO_2 phases. In particular, we hypothesised that Zr containing species cover the rutile

surface sites and in this way prevent formation of harmful copper – rutile connections appeared at high copper loading [12].

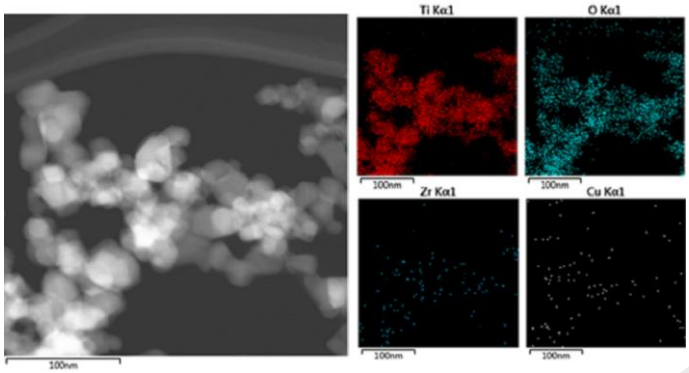

Figure 6. STEM-EDX mapping results for Cu0.1Zr1 modified P25 sample.

To check this hypothesis, titration with Hammett indicators of Cu and Zr modified TiO_2 was applied. The methyl red (MR) colour changes can be caused only by rutile surface sites with $pK_1 = 3.9$. The changes of bromothymol blue (BB) colour can be caused by presence of two surface sites: rutile $pK_1 = 3.9$ and anatase $pK_1 = 4.6$. At the same time, the changes of neutral red (NR) colour can be provoked by the presence of three surface sites: rutile $pK_1 = 3.9$, anatase $pK_1 = 4.6$ and rutile $pK_2 = 6.8$. Following the number of the surface sites determined by titration, we have clearly seen the gradual reduction in number of rutile and anatase acidic sites with modification (Fig. 7). The fraction of anatase and rutile surface sites covered by a modifier was calculated (see supplementary materials); the results are presented in Table 1. The sample with only Cu-loading showed gradual coverage of both anatase and rutile acidic sites even at high 1 mol% of Cu loading. Meanwhile, the sample with 1 mol% Zr nominal loading exhibits sites with a lower total acid strength ($H_0 \leq +6.0$) and shows total vanishing of rutile sites and much lower coverage

of anatase surface sites. Taking into account that Zr-loading is an order of magnitude in excess compared to the Cu nominal loading in the mixed Cu/Zr sample, it becomes evident that Zr is blocking the rutile surface sites and preventing the formation of Cu-rutile connections. As a consequence, the hindering of rutile surface sites postpones the appearance of reverse charge localisation mechanism to higher Cu loading and facilitates the photocatalytic activity of Cu/Zr modified P25 at 0.1 mol% Cu loading compared to Cu only modified sample.

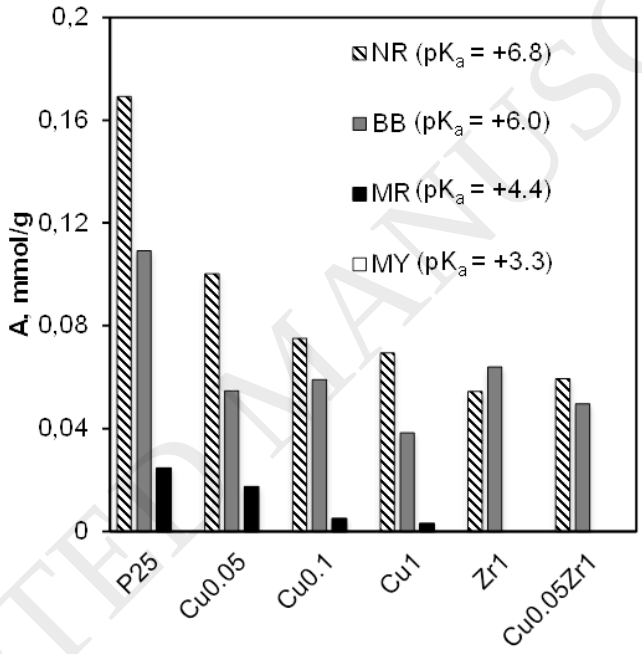

Figure 7. Surface acidity of Cu/Zr modified TiO_2 (NR - neutral red, BB - bromothymol blue, MR - methyl red, MY - methyl yellow).

Interestingly, despite blocking the rutile surface sites, Zr does not influence the photocatalytic activity of P25 toward RB19. There is, therefore, a possibility that the degradation of RB19 proceeds only on the anatase surface sites of P25. However, the presence of a rutile phase cannot be ignored since it has a beneficial role in the charge separation properties of the material.

CONCLUSIONS

Copper/zirconium surface modified photocatalysts were prepared by modification of commercial titanium dioxide Aeroxide® Degussa P25. Hardness testing of the active layers formed from modified TiO_2 showed that Zr loading leads to an improvement in the scratch resistance of the film compared to Cu only modified samples.

Microscopic investigation of the copper modified powders reveal the formation of copper oxide nanoclusters 1-2 nm in size, while EXAFS and STEM-EDX analysis confirm the formation of separate ZrO_2 and CuO species and their homogeneous distribution on the surface of the TiO_2, respectively. Regarding the surface acidic sites, titration revealed that Zr modification results in the total coverage of the rutile surface sites. These together with photocatalytic activity test results strongly support the statement that at high copper loading the formation of copper–rutile connections are harmful.

In the case of combined Cu/Zr modification, Zr acts as a shield, covering the rutile surface that results in copper–anatase interaction. Thereby, zirconium modification beneficially influences the photocatalytic activity of copper modified mixed phase TiO_2 at high copper loading.

Acknowledgements: This research was supported by the Slovenian Research Agency (programs P1-0112, P1-0134), the Belgian-Slovenian project "Development of advanced TiO_2-based photocatalyst for the degradation of organic pollutants from wastewater" and by the project CALIPSOplus under the Grant Agreement 730872 from the EU Framework Programme for Research and Innovation HORIZON 2020. We acknowledge access to the SR facilities of ELETTRA (beamline XAFS, pr.

20165258 and 20160239) and PETRAIII (beamline P65, pr. I-20160044 EC and I-20170160 EC) at DESY, a member of the Helmholtz Association (HGFW). We would like to thank Edmund Welter of PETRA III, and Giuliana Aquilanti, Clara Guglieri and Luca Olivi of ELETTRA for assistance during the experiment.

References

[1] C. Dette, M.A. Pérez-Osorio, C.S. Kley, P. Punke, C.E. Patrick, P. Jacobson, F. Giustino, S.J. Jung, K. Kern, TiO_2 anatase with a bandgap in the visible region, Nano Lett. (2014). doi:10.1021/nl503131s.

[2] M. Xu, S. Shao, B. Gao, J. Lv, Q. Li, Y. Wang, H. Wang, L. Zhang, Y. Ma, Anatase (101)-like structural model revealed for metastable rutile TiO_2 (011) surface, ACS Appl. Mater. Interfaces. (2017). doi:10.1021/acsami.6b16449.

[3] G. Li, N.M. Dimitrijevic, L. Chen, T. Rajh, K. a. Gray, Role of surface/interfacial Cu^{2+} sites in the photocatalytic activity of coupled $CuO{-}TiO_2$ nanocomposites, J. Phys. Chem. C. 112 (2008) 19040–19044. doi:10.1021/jp8068392.

[4] M. Janczarek, E. Kowalska, On the origin of enhanced photocatalytic activity of copper-modified titania in the oxidative reaction systems, Catalysts. (2017). doi:10.3390/catal7110317.

[5] H. Irie, S. Miura, K. Kamiya, K. Hashimoto, Efficient visible light-sensitive photocatalysts: Grafting Cu(II) ions onto TiO_2 and WO_3 photocatalysts, Chem. Phys. Lett. (2008). doi:10.1016/j.cplett.2008.04.006.

[6] H. Irie, K. Kamiya, T. Shibanuma, S. Miura, D.A. Tryk, T. Yokoyama, K. Hashimoto, Visible light-sensitive Cu(II)-grafted TiO_2 photocatalysts: Activities and X-ray absorption fine structure analyses, J. Phys. Chem. C. 113 (2009) 10761–10766. doi:10.1021/jp903063z.

[7] N. Helaïli, Y. Bessekhouad, A. Bouguelia, M. Trari, Visible light degradation of Orange II using xCu_yO_z/TiO_2 heterojunctions, J. Hazard. Mater. (2009). doi:10.1016/j.jhazmat.2009.02.066.

[8] M. Nolan, A. Iwaszuk, H. Tada, Molecular metal oxide cluster-surface modified titanium(iv) dioxide photocatalysts, Aust. J. Chem. 65 (2012) 624–632. doi:10.1071/CH11451.

[9] M. Liu, R. Inde, M. Nishikawa, X. Qiu, D. Atarashi, E. Sakai, Y.

Nosaka, K. Hashimoto, M. Miyauchi, Enhanced photoactivity with nanocluster-grafted titanium dioxide photocatalysts, ACS Nano. 8 (2014) 7229–7238. doi:10.1021/nn502247x.

[10] O. Pliekhova, I. Arčon, O. Pliekhov, N.N. Tušar, U.L. Štangar, Cu and Zr surface sites in the photocatalytic activity of TiO_2 nanoparticles, Environ. Sci. Pollut. Res. 24 (2017) 12571–12581. doi:10.1007/s11356-016-7685-y.

[11] T. Čižmar, U. Lavrenčič Štangar, M. Fanetti, I. Arčon, Effects of different copper loadings on the photocatalytic activity of TiO_2 - SiO_2 Prepared at a low temperature for the oxidation of organic pollutants in water, ChemCatChem. 10 (2018) 2982. doi:10.1002/cctc.201800249.

[12] Q. Jin, M. Fujishima, A. Iwaszuk, M. Nolan, H. Tada, Loading effect in copper(II) oxide cluster-surface-modified titanium(IV) oxide on visible- and UV-light activities, J. Phys. Chem. C. 117 (2013) 23848–23857. doi:10.1021/jp4085525.

[13] L. Yuliati, W. Ruu Siah, N.A. Roslan, M. Shamsuddin, H. O. Lintang, Modification of titanium dioxide nanoparticles with copper oxide co-catalyst for photocatalytic degradation of 2,4-dichlorophenoxyacetic acid, Malaysian J. Anal. Sci. (2016). doi:10.17576/mjas-2016-2001-18.

[14] P. Zawadzki, A.B. Laursen, K.W. Jacobsen, S. Dahl, J. Rossmeisl, Oxidative trends of TiO_2 - hole trapping at anatase and rutile surfaces, Energy Environ. Sci. 5 (2012) 9866–9869. doi:10.1039/c2ee22721e.

[15] F.U. Xianzhi, L.A. Clark, Q. Yang, M.A. Anderson, Enhanced photocatalytic performance of titania-based binary metal oxides: TiO_2/SiO_2 and TiO_2/ZrO_2, Environ. Sci. Technol. 30 (1996) 647–653. doi:10.1021/es950391v.

[16] N. Venkatachalam, M. Palanichamy, B. Arabindoo, V. Murugesan, Enhanced photocatalytic degradation of 4-chlorophenol by Zr^{4+} doped nano TiO_2, J. Mol. Catal. A Chem. 266 (2007) 158–165. doi:10.1016/j.molcata.2006.10.051.

[17] N. Vodišek, K. Ramanujachary, V. Brezová, U. Lavrenčič Štangar, Transparent titania-zirconia-silica thin films for self-cleaning and photocatalytic applications, Catal. Today. 287 (2016) 142–147. doi:10.1016/j.cattod.2016.12.026.

[18] K. Kontapakdee, J. Panpranot, P. Praserthdam, Effect of Ag addition on the properties of Pd–Ag/TiO_2 catalysts containing different TiO_2 crystalline phases, Catal. Commun. 8 (2007) 2166–2170. doi:10.1016/J.CATCOM.2007.03.003.

[19] N. Riaz, F.K. Chong, Z.B. Man, M.S. Khan, B.K. Dutta, Photodegradation of orange II under visible light using Cu-Ni/TiO_2:

Influence of Cu: Ni mass composition, preparation, and calcination temperature, Ind. Eng. Chem. Res. (2013). doi:10.1021/ie303255v.
[20] M.A. Behnajady, H. Eskandarloo, Silver and copper co-impregnated onto TiO_2-P25 nanoparticles and its photocatalytic activity, Chem. Eng. J. (2013). doi:10.1016/j.cej.2013.04.110.
[21] R.I. Bickley, T. Gonzalez-Carreno, J.S. Lees, L. Palmisano, R.J.D. Tilley, A structural investigation of titanium dioxide photocatalysts, J. Solid State Chem. (1991). doi:10.1016/0022-4596(91)90255-G.
[22] D.C. Hurum, A.G. Agrios, K.A. Gray, T. Rajh, M.C. Thurnauer, Explaining the enhanced photocatalytic activity of Degussa P25 mixed-phase TiO_2 using EPR, J. Phys. Chem. B. 107 (2003) 4545–4549. doi:10.1021/jp0273934.
[23] J. Papp, S. Soled, K. Dwight, A. Wold, Surface acidity and photocatalytic activity of TiO_2, WO_3/TiO_2, and MoO_3/TiO_2 photocatalysts, Chem. Mater. 6 (1994) 496–500. doi:10.1021/cm00040a026.
[24] M. Kete, E. Pavlica, F. Fresno, G. Bratina, U.L. Stangar, Highly active photocatalytic coatings prepared by a low-temperature method, Environ. Sci. Pollut. Res. 21 (2014) 11238–11249. doi:10.1007/s11356-014-3077-3.
[25] B. Ravel, M. Newville, ATHENA, ARTEMIS, HEPHAESTUS: data analysis for X-ray absorption spectroscopy using IFEFFIT., J. Synchrotron Radiat. 12 (2005) 537–41. doi:10.1107/S0909049505012719.
[26] J.J. Rehr, R.C. Albers, S.I. Zabinsky, High-order multiple-scattering calculations of x-ray-absorption fine structure, Phys. Rev. Lett. 69 (1992) 3397–3400. doi:10.1103/PhysRevLett.69.3397.
[27] D. Guerrero-Araque, D. Ramírez-Ortega, P. Acevedo-Peña, F. Tzompantzi, H.A. Calderón, R. Gómez, Interfacial charge-transfer process across ZrO_2-TiO_2 heterojunction and its impact on photocatalytic activity, J. Photochem. Photobiol. A Chem. 335 (2017) 276–286. doi:10.1016/j.jphotochem.2016.11.030.
[28] F.W. Lytle, R.B. Greegor, A.J. Panson, Discussion of x-ray-absorption near-edge structure: Application to Cu in the high- Tc superconductors $La_{1.8}Sr_{0.2}CuO_4$ and $YBa_2Cu_3O_7$, Phys. Rev. B. 37 (1988) 1550–1562. doi:10.1103/PhysRevB.37.1550.
[29] N.B. Castagnola, A.J. Kropf, C.L. Marshall, Studies of Cu-ZSM-5 by X-ray absorption spectroscopy and its application for the oxidation of benzene to phenol by air, Appl. Catal. A Gen. 290 (2005) 110–122. doi:10.1016/j.apcata.2005.05.022.
[30] E.M.C. Alayon, M. Nachtegaal, A. Bodi, M. Ranocchiari, J.A. van Bokhoven, Bis(μ-oxo) versus mono(μ-oxo)dicopper cores in a zeolite for converting methane to methanol: an in situ XAS and

DFT investigation, Phys. Chem. Chem. Phys. 17 (2015) 7681–7693. doi:10.1039/C4CP03226H.

[31] N. Spanos, I. Georgiadou, A. Lycourghiotis, Investigation of rutile, anatase, and industrial titania/water solution interfaces using potentiometric titration and microelectrophoresis, J. Colloid Interface Sci. 172 (1995) 374–382. doi:10.1006/jcis.1995.1267.

Table 1. The fraction (F) of anatase and rutile surface sites covered by a modifier.

Sample	F±5, %		
	pK_1^{Rutile}	$pK_1^{Anatase}$	pK_2^{Rutile}
P25	0	0	0
Cu0.05	29	56	24
Cu0.1	80	36	73
Cu1	88	58	48
Zr1	100	24	100
Cu0.05Zr1	100	42	100